MODELING, SIMULATION AND EXPERIMENTAL ANALYSIS OF CONDUCTED EMI FOR A SWITCHING CELL

Gabriele Grandi [*], *Ugo Reggiani* [*], *Domenico Casadei* [*]

Abstract

This paper deals with electromagnetic interference (EMI) conducted emissions produced by power electronic converters. A switching cell is analyzed and a realistic circuit model which takes account of parasitic inductances and capacitances is considered. The numerical results carried out by PSpice have been validated by tests on an experimental set-up.

Introduction

The increase of the switching speed in power switches requires the investigation of electromagnetic interference phenomena due to high values of *di/dt* and *dv/dt*. In particular, care has to be taken in determining a converter model which should consider HF parameters of circuit elements [1,2].
Some difficulties may arise when evaluating parasitic parameters such as stray inductances of connecting wires, parasitic inductances of DC smoothing capacitors, coupling capacitances between each power switch and the ground (heatsink and case). The values of these parameters can be obtained by measurements, field analysis or both. The theoretical and numerical analysis carried out on realistic circuit models of power converters allows the dynamic behavior including conducted EMI to be predicted [3,4].
The influence of the switching speed on EMI and converter losses has been analyzed in [5,6]. Usually the switching speed is chosen by a compromise between high values (low losses, high EMI) and low values (high losses, low EMI) on the basis of the desired converter features. For an accurate design of the converter according to electromagnetic compatibility (EMC) requirements and emission limits, it is necessary to

[*] ***Dip.to di Ingegneria Elettrica, Viale Risorgimento 2, 40136 - BOLOGNA (Italy)***
Tel: +39 51 6443571, Fax: +39 51 6443588, E-Mail: elettrot5@ingbo1.cineca.it

predict the frequency spectrum of the voltage and current. If EMC requirements are not satisfied, it is necessary to modify the layout of the converter or to insert specific reactive components or to design an appropriate input filter [1,2].
The aim of this paper is to present a detailed circuit model of a switching cell that is the basic structure of most power converters. The correct value of every electric parameter can be obtained by measurements or theoretical approach. Utilizing the proposed model it is possible to perform numerical simulations with PSpice and so to emphasize the influence of each HF parameter on conducted emissions. The model has been validated by comparing the calculated results with experimental data. Two line impedance stabilization networks (LISN) have been used in experimental tests and simulations in order to standardize the results.

Fig. 1 - *Basic structure of the switching cell.*

Realistic model of the switching cell

The basic structure of the considered switching cell is depicted in Fig. 1. For an accurate EMC analysis of the cell behavior it is necessary to take HF parasitic components into account. Fig. 2 shows the cell equivalent circuit with the parasitic components, which are

- *Parasitic inductances of the input capacitors*.
  Typical values are 1-10 nH for ceramic capacitors and 30-100 nH for large electrolytic capacitors. A parallel connection of both capacitor types is usually employed in order to obtain a large equivalent capacitance with a low equivalent parasitic inductance. The values of these inductances depend on the internal structure of the capacitors and are usually obtained by measurements being their theoretical calculation a hard task.
- *Stray inductance of the connecting wires.*
  This parameter affects the total inductance of the circuit and is strongly dependent on the converter layout. Typical values for power switch leads are 5-30 nH. The inductance of the connecting wires can be calculated by a general formula valid for circuits having any plane figure [7].

- *Parasitic capacitances between the cell and the ground.*
  The ground potential is introduced by the power switch heatsink and the metallic case. As a consequence, capacitances between the cell and the ground have to be considered in the equivalent circuit. The capacitance values depend on both the converter layout and the power switch geometry. Usually they can be measured or calculated by the formula of the parallel-plate capacitor.

The basic cell shown in Fig. 1 contains a branch consisting of two power MOSFETs. The device M1 performs the switching function and the intrinsic diode of the device M2 provides the free-wheeling path. PSpice models have been used for the numerical simulation of both these elements. The effects of the MOSFET internal capacitances are included in PSpice models, whereas the values of the internal inductances are given by the data sheet and have to be introduced in the circuit model of the switching cell. The values of the main parameters used for the numerical analysis are given in the Appendix.

Fig. 2 - *Cell equivalent circuit with parasitic components.*

The PSpice simulator has been chosen according to the aim of this paper, which does not require the use of very accurate models for power switches. More accurate models can be found in literature (i.e. Power Diode [8], MOSFET and IGBT [9]), but the complexity of their equivalent circuits introduces difficulties in the handling of the cell equivalent circuit, without significant improvements in EMC analysis.

Numerical results

In the measurement procedure of conducted emissions, line impedance stabilization networks (LISN) have to be employed. In order to compare the simulations with the experimental results, it is so necessary to introduce in the simulation circuit two LISNs (50/250μH, 20A-500V), as it is shown in Fig. 2. The topology and the parameter values of the adopted LISN are given in Fig. 3 and Tab. I.

R_m=	50	Ω (Analyz.)
R_b=	5	Ω
R_a=	100	kΩ
C_m=	.33	μF
C_a=	.47	μF
C_b=	8	μF
L_1=	250	μH
L_2=	50	μH

Tab. I - *LISN Parameters*

Fig. 3 - *Circuit topology of the adopted LISN*

The behavior of the chopper has been investigated assuming a switching frequency of 10 kHz and a duty-cycle of 60% in all cases. The power switches are two IRFP460 MOSFET with intrinsic free-wheeling diode and have been modeled by the PSpice component library.

The simulation of the ideal circuit represented in Fig. 1 has been carried out. Figs. 4(a) and 4(b) show the spectrum of the conducted emission across the LISN, for two different switching times of the MOSFET obtained by two different values of the driver resistance (15 Ω and 50 Ω).

The typical conducted EMI frequency range is 150 kHz - 30 MHz. We have considered a slightly wider frequency range (100 kHz - 40 MHz) in order to examine the resonant phenomena completely as explained below.

Comparing Figs. 4(a) and 4(b) we can notice that the higher value of the switching time determines a slight decrease of the disturbance amplitude for frequencies above about 5 MHz.

In order to analyze the influence of the different parasitic components in the realistic equivalent circuit of Fig. 2, the heatsink and the case have been at first considered disconnected from ground. Fig. 5(a) shows the conducted emission spectrum obtained with the parameter values given in Appendix. The switching time is the same as in Fig. 4(a).

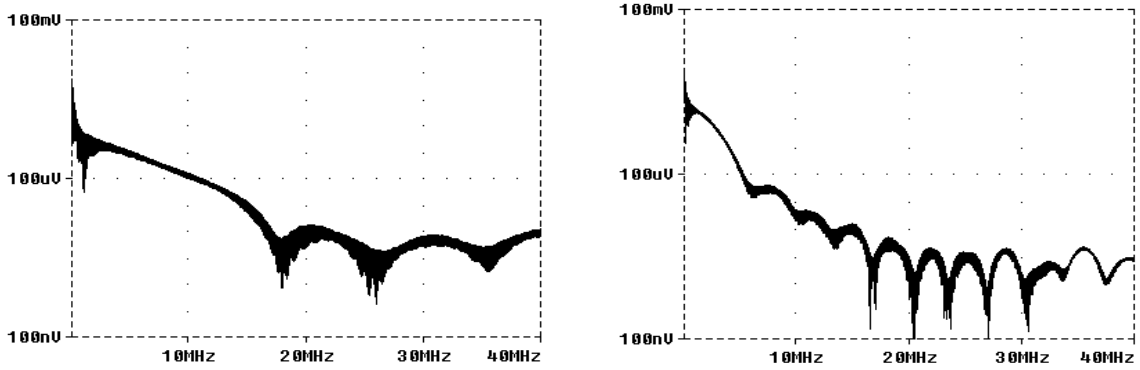

(a) *(b)*

Fig. 4 - *Calculated spectrum of the ideal circuit: (a) rise time 100 ns, fall time 200 ns (b) rise time 300 ns, fall time 600 ns*

As it is possible to see, the spectrum emphasizes the presence of two resonant frequencies of about 709 kHz and 31.8 MHz with an amplitude of 95 dBμV and 60 dBμV, respectively. It has been verified that the higher resonant frequency is due to the series-resonant loop which contains the power switches and the ceramic capacitor. It should be noted that the value of this resonant frequency is practically not affected by the capacitance of the ceramic capacitor, as it is connected in series with the internal capacitance of the off-state power switch, which is characterized by much lower value (i.e. 800 pF versus 0.33 μF).
The lower resonant frequency is related to the loop consisting of the ceramic and electrolytic capacitors, their internal parasitic components and the stray inductance of the connecting wires.
Connecting the heatsink and the case to ground, the cell equivalent circuit changes and, consequently, a different conducted emission spectrum should be expected. The calculated results are shown in Fig. 5(b), in which it is possible to clearly observe a further resonant frequency of about 12.3 MHz with an amplitude of 74 dBμV. This frequency of resonance is introduced by the connection of the heatsink and the LISNs to ground. The corresponding series-resonant circuit consists of the parasitic capacitances between the cell and the ground and the stray inductances of the connecting wires between the cell and the LISNs.

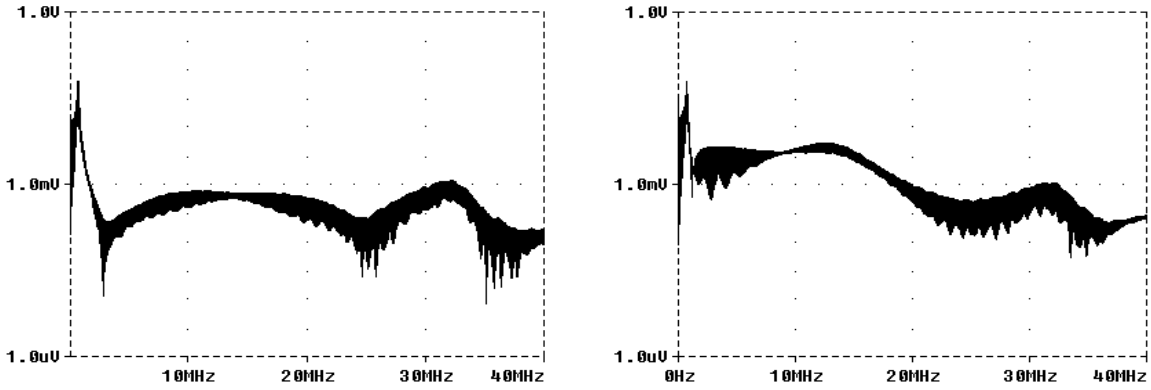

(a) *(b)*

Fig. 5 - *Calculated spectrum: (a) heatsink non-connected to ground (b) heatsink connected to ground*

The previous considerations have been confirmed by the results illustrated in Figs. 6(a) and 6(b), related to the case of heatsink non-connected to ground. In particular, Fig. 6(a) has been determined assuming a zero value for the stray inductance of the connecting wire of the electrolytic capacitor, $L_{wc} = 0$. Fig. 6(b) has been obtained increasing the stray inductance, L_{sd}, of the external connection wire between the MOSFETs from zero to 30 nH. In the former case (Fig. 6a), a reduction in the total inductance of the resonant loop containing the smoothing capacitors causes an increase of the lower resonant frequency from 709 kHz to 1.33 MHz and a decrease of its amplitude from 95 dBμV to 77 dBμV. In the latter case (Fig. 6b), an increase in the overall stray inductance of the loop including the power switches and the ceramic capacitor determines a decrease of the higher resonant frequency from 31.8 MHz to 22.7 MHz and an increase of its amplitude from 60 dBμV to 66 dBμV.

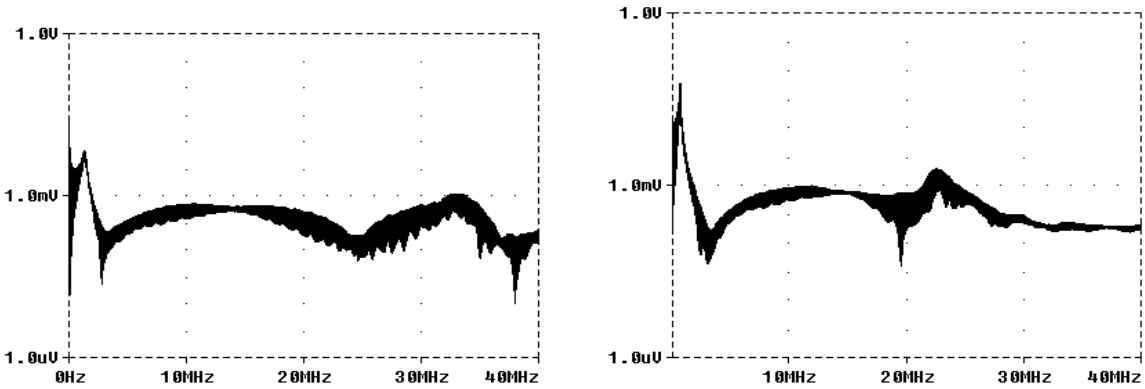

(a) *(b)*

Fig. 6 - *Calculated spectrum with heatsink non-connected to ground:* *(a)* $L_{cw} = 0$ *(b)* $L_{sd} = 30$ *nH*

These results can be verified by the well-known formula for a first-order resonant loop with a series-equivalent capacitance C_{eq} and a series-equivalent inductance L_{eq}

$$f_o = \frac{1}{2\pi\sqrt{L_{eq}C_{eq}}}$$

Experimental results

In order to verify the results obtained by simulating the proposed model with PSpice, a chopper was realized according to the scheme of Fig. 1. The experimental set-up includes two power MOSFET IRFP460 (500V-20A) and an input filter composed by an electrolytic capacitor in parallel with a ceramic capacitor. The parameter values of these elements are reported in Appendix. The chopper was supplied by a DC source (battery) of 100V and an ohmic load of 20 Ω was connected to the output.
For the experimental tests, an HP 8590 Spectrum Analyzer was employed in the same frequency range considered in the previous PSpice simulations (100 kHz - 40 MHz).
Fig. 7(a) shows the peak spectrum envelope of the conducted emission measured in the same operating conditions of Fig. 5(a). A good agreement was achieved between the numerical and experimental results which clearly show the two resonant frequencies of 700 kHz, 93 dBμV and 32.1 MHz, 68 dBμV, respectively.
Fig. 7(b) illustrates the peak spectrum envelope measured with the heatsink connected to ground. In this case two further resonant frequencies are introduced. The higher one occurs at the frequency of 12.1 MHz with an amplitude of 75 dBμV. It is very close to the corresponding resonant frequency obtained by the simulation (12.3 MHz, 74 dBμV). The lower resonant frequency is about 4 MHz but its amplitude does not match the value obtained by the simulation in a satisfactory way.
The experimental results show that the equivalent circuit used for the switching cell simulation allows the main conducted EMI phenomena to be predicted with sufficient accuracy.

(a) *(b)*

Fig. 7 - *Measured peak spectrum envelope: (a) heatsink non-connected to ground (b) heatsink connected to ground*

Conclusions

In this paper, an analysis has been developed in order to emphasize how conducted emissions are generated in a switching cell. For this purpose a detailed equivalent circuit has been proposed. This model permits the influence of the different parasitic components to be predicted. The main results of the numerical and experimental analysis can be summarized as follows

- the parasitic capacitance of the electrolytic capacitor has in practice no influence on the resonant frequencies, since it is always connected in series with capacitances having much lower values,
- the parasitic capacitance of the ceramic capacitor practically affects only the lowest resonant frequency in the considered EMI frequency range,
- the internal capacitances of the power switches influence the highest resonant frequency in the considered EMI frequency range,
- the parasitic capacitances between the heatsink and the ground cause further resonant frequencies,
- the parasitic inductances of the input capacitors and the internal inductances of the power switches do not affect the resonant frequencies, which are introduced by the connection of the heatsink to ground. This is due to the much higher value of the inductance of the connecting wire between the heatsink and the ground.

References

[1] P.A.Chatterton, M.A.Houlden "*EMC Electromagnetic theory to practical design*". WILEY 1992, Chichester, West Sussex (UK)

[2] L.Tihanyi "*Electromagnetic compatibility in power electronics*". IEEE Press 1995, New York (USA)

[3] M.Lardellier, G.Rojat, E.Labouré, F.Costa "*EM disturbance in commutation cells for different technologies of silicon components*". **EMC**, 13-16 Sept. 1994, Roma (I), pp. 465-470.

[4] R.Sheich, J.Roudet "*EMI conducted emission in the differential mode emanating from an SCR: phenomena and noise level prediction*". **IEEE Trans. PE**, Vol. 10, N. 2, March 1995, pp. 105-110.

[5] A.Consoli, S.Musumeci, G.Oriti, A.Testa "*An innovative EMI reduction design technique in power converters*". **EMC**, 13-16 Sept. 1994, Roma (I), pp. 459-464

[6] E.Labouré, F.Costa, M.Lardellier, G.Rojat "*Losses/EMI compromise relating to electrical constraints and components technology in static converters*". **EPE**, 18-21 Sept. 1995, Sevilla (E), proc. pp. 3.340-3.345

[7] F.W.Grover "*Inductance calculations*", **Van Nostrand**, New York (USA) - 1946.

[8] F.Bertha, B.Velaerts, E.Tatakis "*An improved power diode model for PSspice, applied to converter simulation*". **EPE**, 13-66 Sept. 1993, Brighton (UK), proc. pp. 249-254.

[9] J.Pilacinski "*A method for determining the parameters of power MOSFET and IGBT transistor models applied in the PSpice program*". **EPE**, 18-21 Sept. 1995, Sevilla (E), proc. pp. 3.356-3.361.

Appendix

CONNECTING WIRES	CAPACITORS	MOSFETS
$R_{w1} = 0.1\ \Omega$	$C_{el} = 3.3\ mF$	$L_{d1} = 5\ nH$
$L_{w1} = 0.2\ \mu H$	$L_{el} = 34\ nH$	$L_{s1} = 5\ nH$
	$R_{el} = 0.03\ \Omega$	$R_{g1} = 15\ (50)\Omega$
$R_{w2} = 0.1\ \Omega$	$R_s = 10\ k\Omega$	$v_{g1} = 0 - 15\ V$
$L_{w2} = 0.2\ \mu H$		
	$C_{ce} = 0.33\ \mu F$	$L_{d2} = 5\ nH$
$R_{wg} = 0.1\ \Omega$	$L_{ce} = 7\ nH$	$L_{s2} = 5\ nH$
$L_{wg} = 0.5\ \mu H$	$R_{ce} = 0.05\ \mu F$	$R_{g2} = 15\ (50)\Omega$
		$v_{g2} = 0 - 15\ V$
$L_{wc} = 100\ (0)\ nH$	$C_{g1} = 50\ pF$	
$L_{sd} = 0\ (30)\ nH$	$C_{g2} = 50\ pF$	

Main parameter values utilized for PSpice simulations